Manganese-superoxide dismutase (MnSOD) rescues redox balance and mucosal barrier function in midgut of hybrid fish (*Carassius cuvieri* ♀ × *Carassius auratus* red var ♂) infected with *Aeromonas hydrophila* and *Edwardsiella tarda*

Jie Ou [a], Wei-Sheng Luo [a], Zi-Rou Zhong [a], Qing Xie [a], Fei Wang [a], Ning-Xia Xiong [a,b], Sheng-Wei Luo [a,*]

[a] *State Key Laboratory of Developmental Biology of Freshwater Fish, College of Life Science, Hunan Normal University, Changsha, 410081, PR China*
[b] *Department of Aquatic Animal Medicine, College of Fisheries, Huazhong Agricultural University, Wuhan, 430070, PR China*

ARTICLE INFO

ABSTRACT

MnSOD is a ubiquitous metalloenzyme that constitutes the first line of antioxidant defense against oxidative stress. In this study, full length sequence of MnSOD was identified from hybrid crucian carp (WR, *Carassius cuvieri* ♀ × *Carassius auratus* red var ♂). Tissue-specific analysis revealed that the highest expression of WR-MnSOD was detected in kidney. *Aeromonas hydrophila* challenge could dramatically enhance WR-MnSOD mRNA expression in tissues. *In vivo* administration of purified WR-MnSOD peptide could maintain gut mucosal barrier function, rescue redox balance as well as decrease apoptotic cell death in midgut upon bacterial infection, suggesting that WR-MnSOD is playing a crucial role in gut mucosal barrier function and could be used as feed additive to improve gut immunity in fish.

1. Introduction

Evidences are emerging that ambient stressors can cause abnormal physiological response in mammals [1]. Similarly, biotic or abiotic stress may directly suppress fish immunity and then render fish less resistant to invasive pathogens [2]. Moreover, pollutants such as antibiotics and heavy metals may enable marked alteration of microbe community to accelerate proportion of resistant pathogens in nature environment [3]. Among documented pathogens, *Aeromonas hydrophila* and *Edwardsiella tarda* are serious gram-negative bacteria that can cause infectious diseases in aquatic organisms by generating a large quantity of virulence factors and bacterial toxins [4]. Previous studies demonstrate that *A. hydrophila* challenge can significantly increase accumulative mortality of allogynogenetic crucian carp [5], whereas *E. tarda* is an intracellular pathogen that can lead to occurrence of edwardsiellosis in farmed fish characterized by exophthalmia, ascites and severe lesions of the internal organs [6].

Crucian carp (*Carassius auratus*) is one of popular farmed fish species in China, which is due to its delicious taste and high stress resistance [7]. Currently, global climate change may lead to environmental degradation and then exacerbate risk factors for emerging diseases in aquaculture [8]. Although teleost fish commonly possess immune factors such as pathogen recognizing receptors (PRRs) to participate in elimination of invasive pathogens [9], some pathogens can effectively avoid host immunity to breach mucosal barrier for deeper infection [10]. Among known antibacterial molecules, reactive oxygen species (ROS) can exhibit a strong bactericidal activity within the host, but its prolonged generation can promote antioxidant insult and impair macromolecular bioactivity [11]. Manganese-superoxide dismutase (MnSOD) is one of crucial SOD enzymes primarily found in mitochondria, which can lessen the deleterious effect of super oxide radicals derived from mitochondrial components [12]. MnSOD may also be involved in immune responsive mechanism under the exposure to a wide range of stimulatory factors such as LPS and cytokines [13]. Recent findings indicate that overexpression of human MnSOD can confer protection against ionizing radiation damage in small intestine of mice [14]. However, the study on its immunoregulatory function in midgut of hybrid fish following bacterial infection is unclear.

In this study, the aims were to characterize architectures of MnSOD in hybrid crucian carp. The expression profiles of MnSOD in immune-

---

Table 1
The primer sequences used in this study.

Primer names	Sequence direction (5' → 3')	Use
qpcr-occludin-F	GTTGCCCATCCGTAGTTCAGT	qPCR
qpcr-occludin-R	CTTCAGCCCAGACGCTTGTTG	qPCR
qpcr-claudin7-F	GCCCTCTGTAGCATTGTCGC	qPCR
qpcr-claudin7-R	GCCTCCACCCATTATGTCCA	qPCR
qpcr-claudin8- F	GAGCAGGTGAAGCACGAGAA	qPCR
qpcr-claudin8- R	CGGGAGGAACAGCAGGG	qPCR
qpcr-claudin12- F	CTTGCTGCTCCAAAACTCCTG	qPCR
qpcr-claudin12- R	GCCACATACACCCCAAACTCT	qPCR
qpcr-TrxR-F	TCCTGGGGTCTGGGTGG	qPCR
qpcr- TrxR-R	CAGCCGAACTTGCGTGC	qPCR
qpcr-OXR1-F	CATCAGGCAGCATTAGAGGC	qPCR
qpcr- OXR1-R	TGGAGGGGATTTTAGGTTTTG	qPCR
qPCR-TXNL-F	TGATGCCGTTCGTCAGTAAAG	qPCR
qPCR- TXNL-R	GGTTGATTGAAGGCGATTGTG	qPCR
qpcr-caspase3-F	AGATGCTGCTGAGGTCGGG	qPCR
qpcr- caspase3-R	GGTCACCACGGGCAACTG	qPCR
qpcr- caspase8-F	TGTGAATCTTCCAAAGGCAAA	qPCR
qpcr- caspase8-R	CTGTATCCGCAACAACCGAG	qPCR
qpcr-NR13-F	GGCTGGAGGAAAACGGAG	qPCR
qpcr-NR13-R	AACAGTGCGGTCTTCATCG	qPCR
qpcr-Bcl2-F	AGCCGCAGTATTGTGGTGA	qPCR
qpcr- Bcl2-R	CATTTCCGCAAAGTCCGA	qPCR

related tissues were investigated following *A. hydrophila* challenge. After that, MnSOD fusion protein was generated *in vitro* and then its immunoregulatory effect on gut mucosal barrier function was studied, providing a new insight into the regulatory function of MnSOD in hybrid fish.

2. Materials and methods

2.1. Ethics approval

All applicable international, national, and/or institutional guidelines for the care and use of animals were followed. We followed the laboratory animal guideline for the ethical review of the animal welfare of China (GB/T 35892–2018).

2.2. Animals

Hybrid crucian carp (WR) was generated by crossing white crucian carp (*Carassius cuvieri*, WCC, ♀) and red crucian carp (*Carassius auratus* red var, RCC, ♂). Healthy WRs (approximately 19.81 ± 3.75 g) were obtained from a fishing base in Changsha, China. Then, fish were acclimatized in aquarium for two weeks and fed with commercial diet
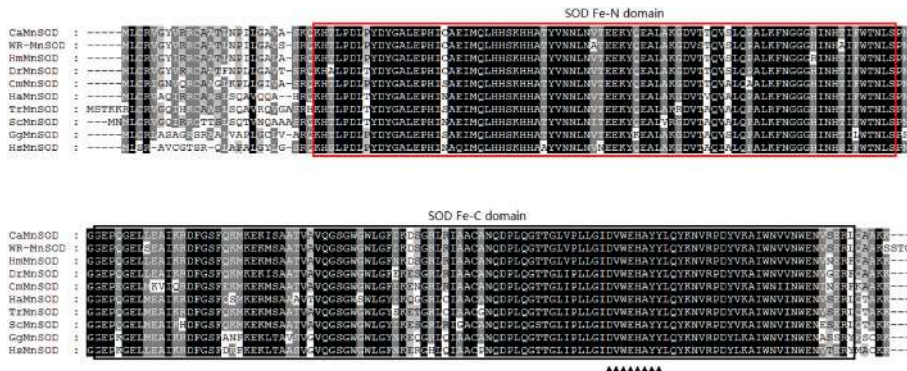
Fig. 1. Bioinformatics analysis of WR-MnSOD. (A) Multiple alignment of the predicted amino acid sequence of WR-MnSOD with other MnSOD sequences. The shared residues represented the similar regions between the different species and the conservative degree was distinguished from light to dark. (B) Phylogenetic tree constructed by using full-length amino acid sequences of MnSOD. Full-length MnSOD amino acid sequences were extracted from Genbank and analyzed by using Neighbor-Joining method by Mega 6.0 with 1000 bootstrap replications. The numbers shown at branches indicated the bootstrap values (%).
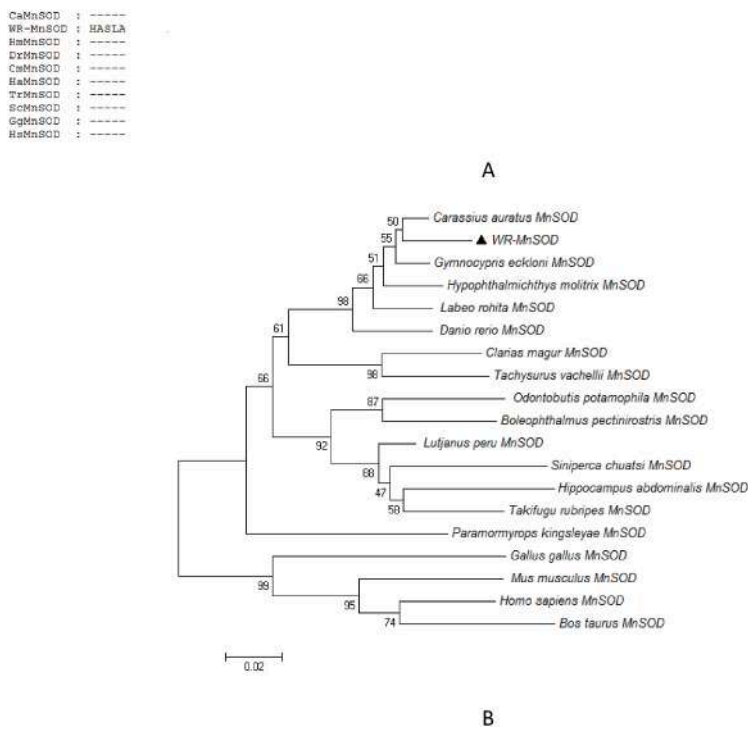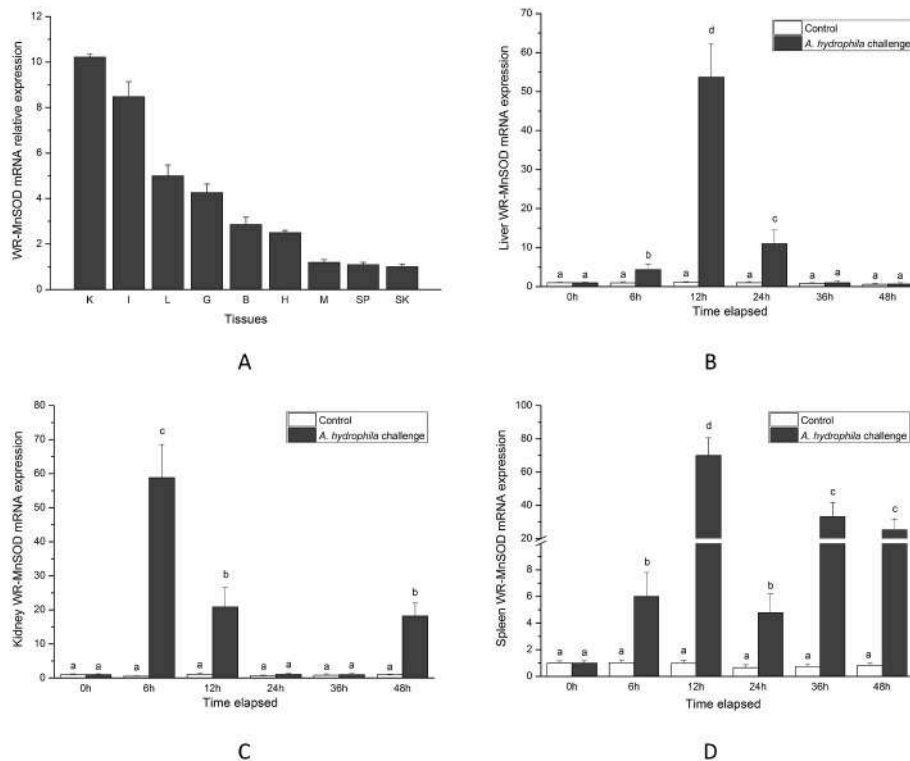
Fig. 2. Gene expression levels of WR-MnSOD. (A) Tissue-specific expressions determined by qRT-PCR assay. L: liver; K: kidney; SP: spleen; SK: skin; H: heart; G: gill; B: brain; I: intestine; M: muscle. (B–D) Expressions of WR-MnSOD were detected in liver, kidney and spleen at 0, 6, 12, 24, 36 and 48 h post-challenge. The calculated data (mean ± SD) with different letters were significantly different (P < 0.05) among the groups. The experiments were performed in triplicate.

twice daily till 24 h before challenge experiment. The excess of dietary feed and fish feces were cleaned up and one-third of water was replaced with clean freshwater in every three days in order to maintain water quality and avoid pathogenic contamination during fish accumulation or challenge experiment. Then, both fish infection experiment and subsequent analysis contained three biological replicates.

2.3. Infection with A. hydrophila

A. hydrophila (L3-3 strain, OM184261) was cultured in Luria-Bertani (LB) medium at 28 °C for 24 h, centrifuged at $12000 \times g$ and resuspended in 1 × PBS (pH 7.3, Sangon Biotech, Shanghai, China) before challenge experiment. Intraperitoneal injection of *A. hydrophila* (1×10^7 CFU ml^{-1}) served as *A. hydrophila* infection group, while equivalent volume of sterile PBS injection was used as control group. Tissues were isolated at 0, 6, 12, 24, 36 and 48 h post-injection, immediately frozen in liquid nitrogen and preserved in −80 °C. Each group contained three biological replicates, respectively.

2.4. Gene cloning, bioinformatics analysis and plasmid construction

Based on previous studies, open reading frame (ORF) sequence of WR-MnSOD was cloned [15]. After that, domain architectures and binding sites were analyzed by NCBI blast, SignalP 5.0 server and TMHMM 2.0 server, while phylogenetic analysis was constructed by using MEGA 6.0. Additionally, ORF sequence were ligated to pET32a plasmid and then transformed into *Escherichia coli* BL21 (DE3) competent cells for fusion protein production. Positive bacterial clone was subjected for sequencing confirmation (Tsingke, Beijing, China).

2.5. Prokaryotic expression, purification and western blotting of WR-MnSOD

Generation and purification of fusion proteins were performed as

described previously [16]. The above *E. coli* BL21 clones inserted with corrected pET32a plasmids were cultured until OD600 value reached about 0.6, then 1 mM IPTG was added for another 4 h incubation. Pellets were harvested for sonication treatment, dissolved in urea-containing buffer. After centrifugation, supernatant proteins were purified by using Ni-NTA resins (Thermo Fisher Scientific, Shanghai, China). After dialysis, purified WR-MnSOD fusion protein was validated by western blotting [17]. Purified WR-MnSOD fusion protein was loaded on SDS-PAGE gel, separated electrophoretically and transferred to PVDF membranes. After incubation with blocking buffer, membranes were reacted with 1:2000 diluted His-tag antibody and enzyme-conjugated secondary antibody, respectively. Finally, PVDF membranes were developed and visualized.

2.6. Gut perfusion assay

Gut perfusion assay was performed as described previously [18,19]. In brief, *A. hydrophila* L3-3 and *E. tarda* I1-4 strain were cultured in Luria-Bertani (LB) medium at 28 °C for 24 h and resuspended in 1 × PBS before use. Firstly, fish were anally intubated with WR-MnSOD fusion protein (0.15 mg/per fish) by using a gavage needle inserted into a depth of approximately 3 cm, while equivalent per gram of pET32a tag was used as control group, respectively. Following treatment with above recombinant proteins for 48 h, the above pretreated WRs were anally intubated with *A. hydrophila* (L3-3 strain, OM184261) or *E. tarda* (I1-4 strain, OM190416) at the dose of 1×10^8 CFU ml^{-1}, which is used as pET32a + *A. hydrophila* group, pET32a + *E. tarda* group, WR-MnSOD + *A. hydrophila* group and WR-MnSOD + *E. tarda* group, respectively. After that, tissues were isolated at 24 h post-infection, then immediately frozen in liquid nitrogen and preserved in −80 °C. Each group contained three biological replicates, respectively.
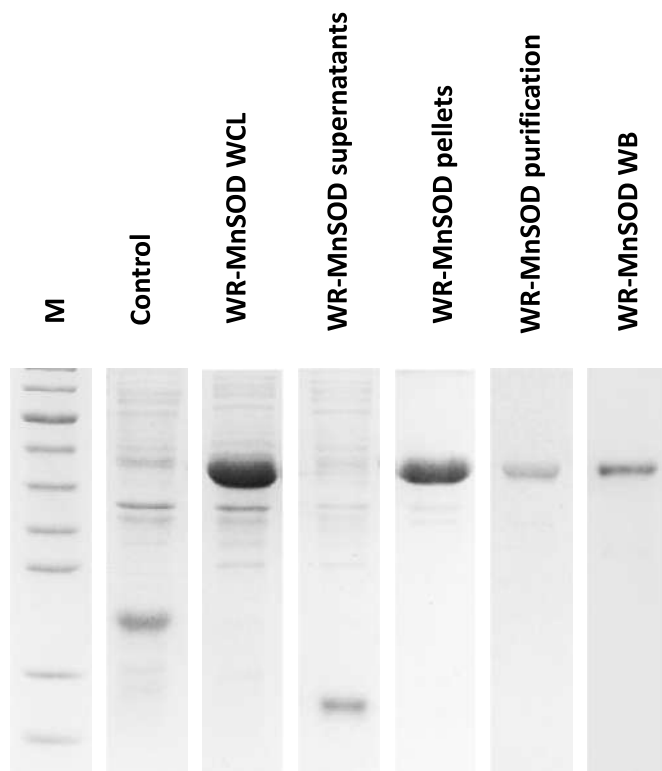
Fig. 3. Generation and validation of WR-MnSOD fusion proteins. Lane M: Protein molecular standard; Lane control: Total protein was isolated from IPTG induced pET32α-BL21; Lane WR-MnSOD WCL: Total protein was isolated from whole cell lysis of pET32α-WR-MnSOD-BL21; Lane WR-MnSOD supernatants: Supernatants from induced pET32a-WR-MnSOD-BL21; Lane WR-MnSOD pellets: Pellets from induced pET32a-WR-MnSOD-BL21; Lane WR-MnSOD purification: Purified WR-MnSOD fusion protein; Lane WR-MnSOD WB: Purified WR-MnSOD fusion protein was identified using anti-His tag antibody.

2.7. RNA isolation, cDNA synthesis and qRT-PCR assay

Total RNA was extracted from isolated tissues by using HiPure Total RNA Mini Kit (Magen, China). Following quality check, 1000 ng of purified total RNA was used for cDNA synthesis by using MonScript™ RT III All-in-One Mix with dsNase (Monad, China). Relative expressions of occludin, claudin-7, claudin-8, claudin-12, thioredoxin reductase (TrxR), oxidation resistance 1 (OXR1), thioredoxin (TXNL), caspase-3, caspase-8, anti-apoptotic protein NR13 (NR13) and B-cell lymphoma-2 (Bcl-2) were investigated by qRT-PCR assay [20,21]. In brief, qRT-PCR assay was performed by using PowerUp SYBR Green Master Mix (Applied Biosystems, USA). At the end of qRT-PCR assay, melting curve analysis was implemented to confirm credibility of each qRT-PCR result. The primers used in this study were shown in Table 1. 18S rRNA was used as internal control to normalize the results. Primer specificity was confirmed and each sample was analyzed in triplicate to certify the repetitiveness and credibility of experimental results. qRT-PCR results were measured by using Applied Biosystems QuantStudio 5 Real-Time PCR System with $2^{-\triangle\triangle Ct}$ methods.

2.8. Histological analysis

The above anally intubated midgut samples were fixed in Bouin solution, dehydrated in ethanol, clarified in xylene, and embedded in paraffin wax. Then, samples were sectioned (approximately 5 μm thick) and stained by using a hematoxylin-eosin (HE) staining kit (Sangon Biotech, Shanghai, China)) [22]. Prepared slides were observed by using a light microscope with 200 × magnification. The experiment was repeated in triplicate.

2.9. Catalase (CAT) activity

Midgut CAT activities were detected at OD_{405} absorbance by using a CAT activity kit (Nanjing Jiancheng Bioengineering Institute, China). Results were given in units of CAT activity per milligram of protein, where 1 U of CAT is defined as the amount of enzyme decomposing 1 μmol H_2O_2 per second. The experiment was repeated in triplicate.

2.10. Glutathione peroxidase (GPx) activity

Midgut GPx activities were observed at OD_{340} absorbance by using a GPx activity kit (Beyotime Biotechnology, China). Results were shown as mU GPx activity per milligram of protein. The experiment was repeated in triplicate.

2.11. Glutathione reductase (GR) activity

Midgut GR activities were detected at OD_{412} absorbance by using a GR activity kit (Beyotime Biotechnology, China). Results were presented as mU GR activity per milligram of protein. The experiment was repeated in triplicate.

2.12. Statistical analyses

SPSS program was used for data calculation, which is subjected to one-way ANOVA. If the analytical levels reach less-than 0.05 P-value, results were statistically significant.

3. Results

3.1. Characterization of WR-MnSOD sequence

In Fig. 1A, the obtained ORF sequence of WR-MnSOD gene encoded 233 amino acid residues with an estimated molecular mass of 25.72 KDa, possessing a SOD-Fe-N domain, a SOD-Fe-C domain and a conserved characteristic sequence ($D^{185}V^{186}W^{187}E^{188}H^{189}A^{190}Y^{191}Y^{192}$). In Fig. 1B, phylogenetic tree analysis revealed that WR-MnSOD sequence was similar to those of other teleosts, suggesting that the evolutionary relationship was in agreement with the concept of the traditional taxonomy.

3.2. Expression profiles of WR-MnSOD mRNA

In Fig. 2A, tissue-specific WR-MnSOD mRNA expressions were detected in all isolated samples. The highest expression level of WR-MnSOD was observed in kidney, whereas the lowest mRNA expression level was detected in skin. Expression patterns of WR-MnSOD mRNA in liver, kidney and spleen were investigated at 0, 6, 12, 24, 36 and 48 h following *A. hydrophila* challenge. In Fig. 2B, liver WR-MnSOD mRNA expression began to increase at 6 h and peaked at 12 h following *A. hydrophila* challenge with the highest value of 53.62-fold greater than that of the control, followed by a sharp decrease from 24 h to 48 h. In Fig. 2C, a high-level of WR-MnSOD expression in kidney of *A. hydrophila*–infected WR was observed at 6 h with the highest value of 58.73-fold greater than that of the control. In Fig. 2D, WR receiving *A. hydrophila* infection showed a 69.87-fold increase in spleen at 12 h, followed by a sharp fluctuation from 24 h to 48 h.

3.3. Prokaryotic expression and fusion protein validation

In Fig. 3, fusion protein generation was detected in pET32a-WR-MnSOD transformed cells in comparison with that of pET32a transformed cells, respectively. After Ni-NTA purification, the purified WR-MnSOD fusion protein was confirmed by western blotting using anti-His antibody.
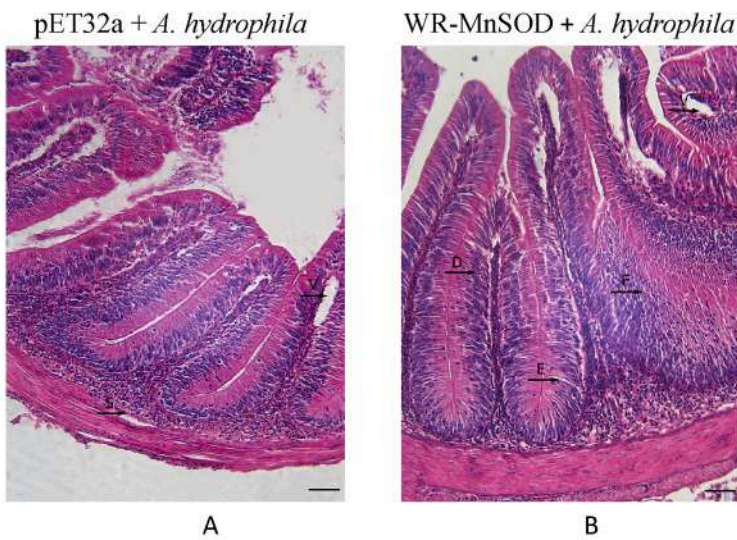
Fig. 4. *In vivo* administration of WR-MnSOD on the Histological characteristics of midgut subjected to *A. hydrophila* infection. (A–B) Midgut tissues were sectioned and stained by using HE staining kit. E: edema of midgut wall; H: goblet cell hyperplasia; D: villi deformation; V: villus vacuolization; S: submucosal rupture; F: villus fusion. (C–D) Average numbers of goblet cells and length-to-width ratio of midgut villi were calculated. The calculated data (mean ± SD) with different letters were significantly different (P < 0.05) among the groups. The experiments were performed in triplicate.
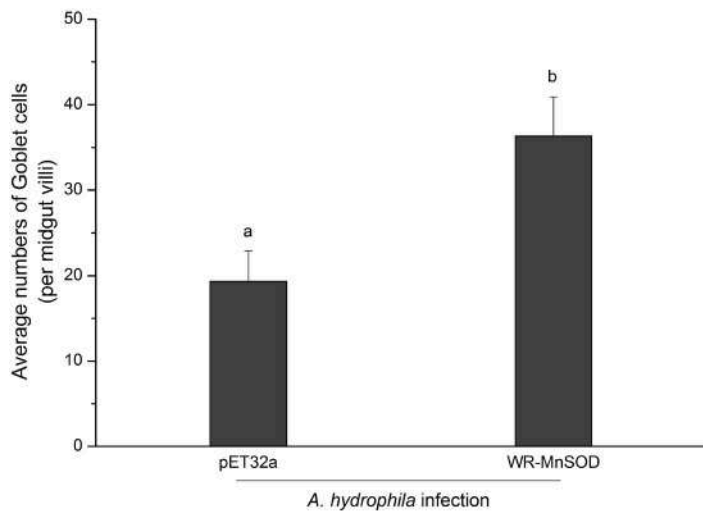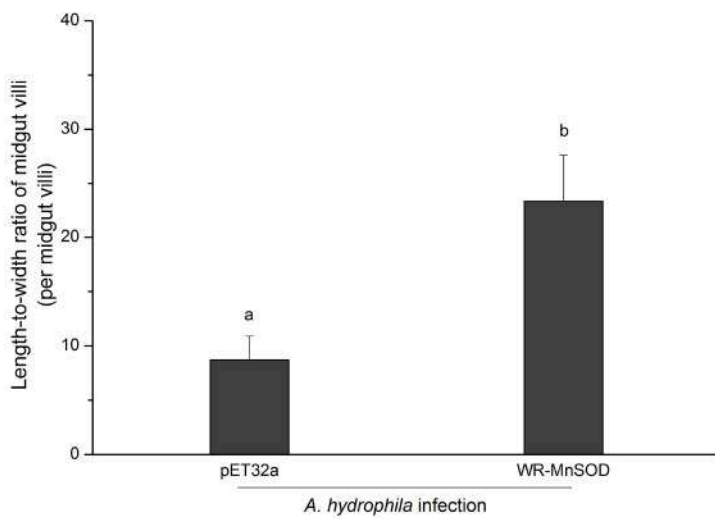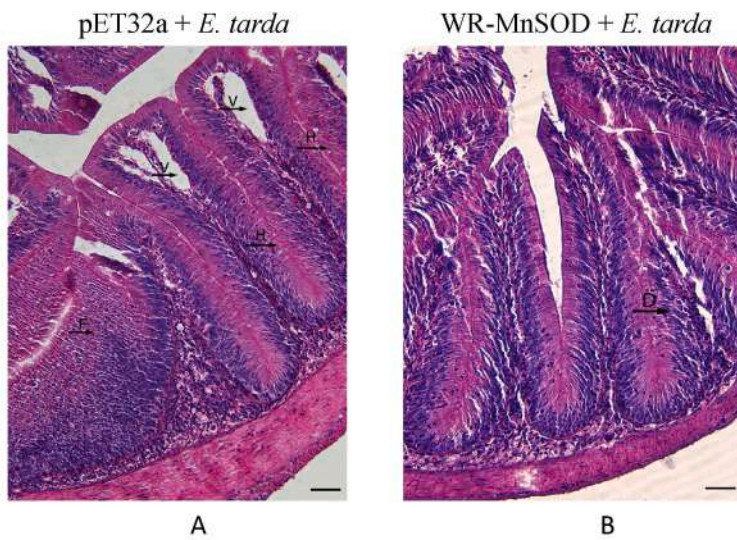
Fig. 5. *In vivo* administration of WR-MnSOD on the Histological characteristics of midgut subjected to *E. tarda* infection. (A–B) Midgut tissues were sectioned and stained by using HE staining kit. E: edema of midgut wall; H: goblet cell hyperplasia; D: villi deformation; V: villus vacuolization; S: submucosal rupture; F: villus fusion. (C–D) Average numbers of goblet cells and length-to-width ratio of midgut villi were calculated. The calculated data (mean ± SD) with different letters were significantly different (P < 0.05) among the groups. The experiments were performed in triplicate.
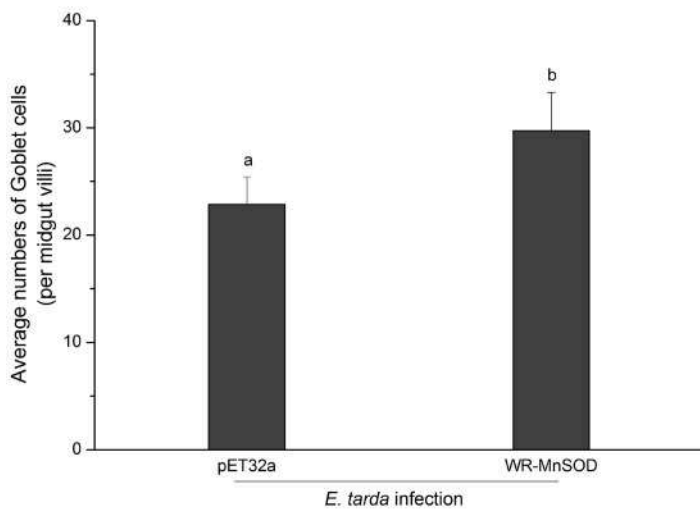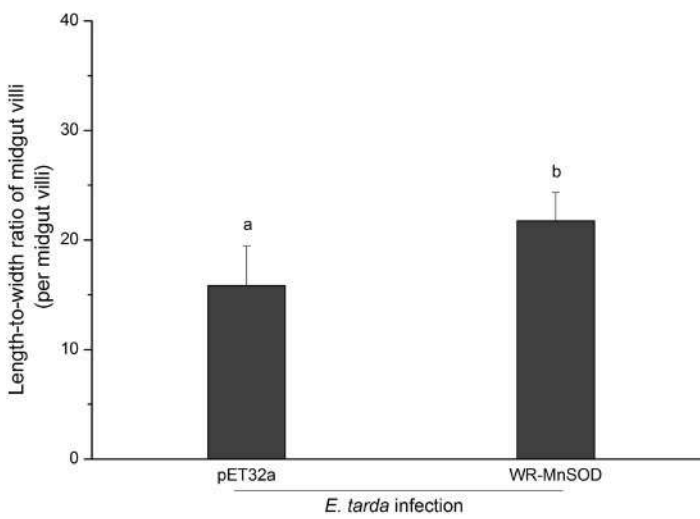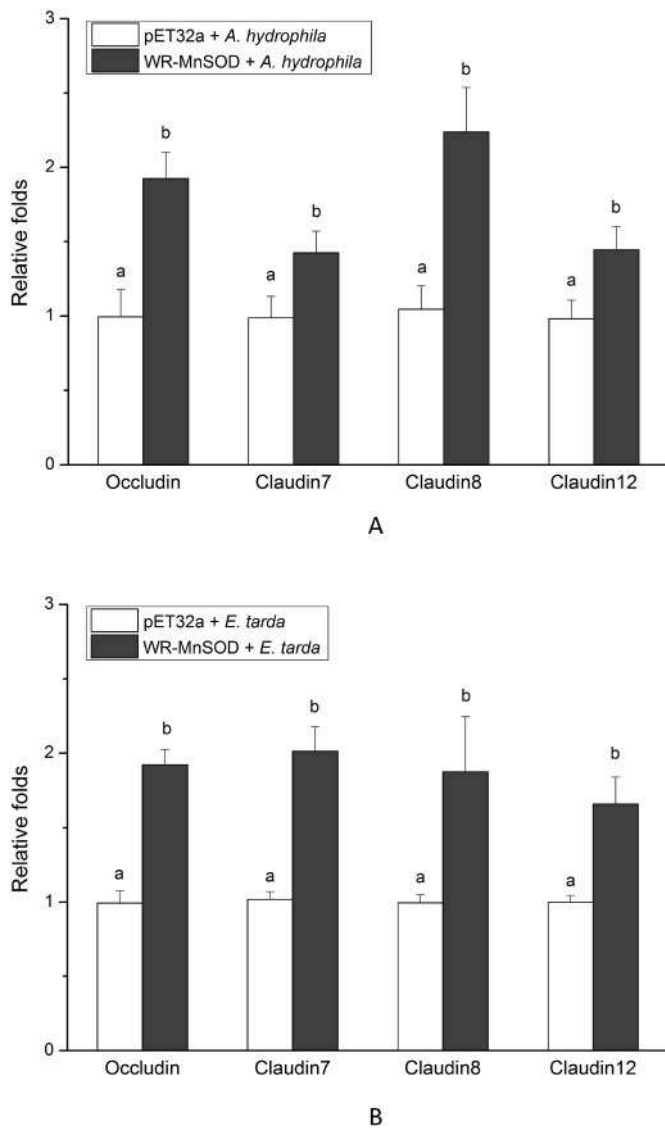
Fig. 6. *In vivo* administration of WR-MnSOD on expressions of tight junction proteins in midgut following *A. hydrophila* and *E. tarda* infection. Expression levels of occludin (A), claudin-7 (B), claudin-8 (C) and claudin-12 (D) were determined in midgut of WR. The calculated data (mean ± SD) with different letters were significantly different (P < 0.05) among the groups. The experiments were performed in triplicate.

3.4. Effect of WR-MnSOD on histological changes in midgut upon bacterial infection

WRs pretreated with recombinant proteins were infected with *A. hydrophila* and *E. tarda*, respectively. As shown in Fig. 4A–B and Fig. 5A–B, midgut villi exhibited a severe pathological characteristics with deformed cell morphology in midgut of *A. hydrophila-* and *E. tarda-*infected fish with increased level of atrophy and rupture, but average numbers of goblet cells and length-to-width ratios of midgut villi were consistently higher in WR-MnSOD + *A. hydrophila* group and WR-MnSOD + *E. tarda* group by comparing with their respective control groups (Fig. 4C-D and Fig. 5C–D).

3.5. Detection of midgut tight junction protein genes and antioxidant prosperities

\Expression levels of occludin, claudin-7, claudin-8, claudin-12, TrxR, OXR1 and TXNL in midgut increased sharply in WR-MnSOD +
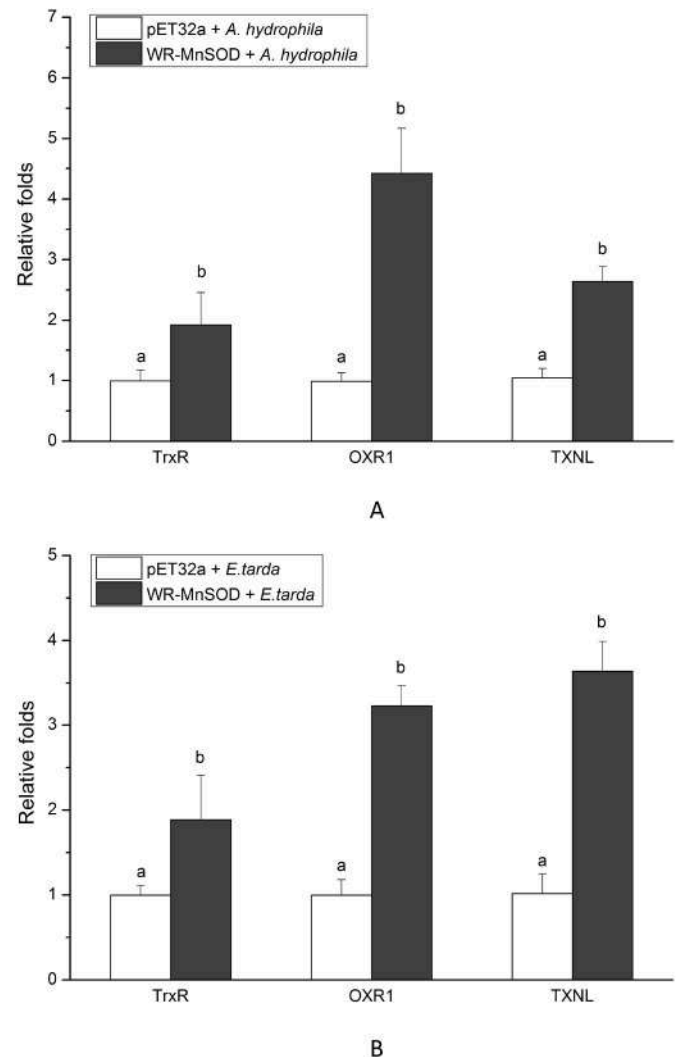
Fig. 7. *In vivo* administration of WR-MnSOD on expressions of antioxidant genes in midgut following *A. hydrophila* and *E. tarda* infection. Expression levels of TrxR (A), OXR1 (B) and TXNL (C) were detected in midgut of WR. The calculated data (mean ± SD) with different letters were significantly different (P < 0.05) among the groups. The experiments were performed in triplicate.

Table 2
Effect of MnSOD administration on Midgut enzyme activity in WR subjected to *A. hydrophila* infection.

Treatments	GR (mU/mg prot)	GPx (mU/mg prot)	CAT (U/mg prot)
pET32a + *A. hydrophila*	24.23 ± 3.57[a]	161.2 ± 25.64[a]	9.11 ± 1.11[a]
WR-MnSOD + *A. hydrophila*	48.75 ± 8.21 [b]	216.32 ± 12.74 [b]	13.38 ± 1.42 [b]

Notes: The calculated data (mean ± SD) with different letters (a, b, c) were significant different (P < 0.05).

A. hydrophila group and WR-MnSOD + *E. tarda* group by comparing with those of the controls, respectively (see Figs. 6 and 7). As shown in Table 2 and Table 3, fish treated with WR-MnSOD exhibited a marked increase of GR, GPx and CAT activity in midgut subjected to *A. hydrophila* infection and *E. tarda* infection, respectively.

3.6. Expressions profiles of apoptosis-related genes

To investigate the protective effect of WR-MnSOD in *A. hydrophila-*

Table 3

Effect of MnSOD administration on Midgut enzyme activity in WR subjected to *E. tarda* infection.

Treatments	GR (mU/mg prot)	GPx (mU/mg prot)	CAT (U/mg prot)
pET32a + *E. tarda*	15.13 ± 2.07^a	77.61 ± 5.64^a	$4.82 \pm 0/93^a$
WR-MnSOD + *E. tarda*	32.48 ± 4.71^b	166.77 ± 21.54^b	17.47 ± 4.42^b

Notes: The calculated data (mean ± SD) with different letters (a, b, c) were significant different ($P < 0.05$).

and *E. tarda*-induced apoptotic cascades, expression profiles of caspase-3, caspase-8, NR13 and Bcl-2 were detected at 24 h post-infection.

In Fig. 8A-F, *in vivo* administration of WR-MnSOD fusion protein could dramatically attenuate expressions of caspase-3 and caspase8 in midgut, liver and spleen after infection with *A. hydrophila* and *E. tarda*, while elevated expressions of NR13 and Bcl-2 were observed.

4. Discussion

Increasing studies have demonstrated that bacteria-induced ROS generation is playing an important role in the regulation of signal transduction for bridging innate immunity with adaptive immune response, while its long-term elevation can promote antioxidant insults and impair macromolecular products [23]. Our previous findings have demonstrated that invasive *A. hydrophila* can alleviate antioxidant status and impair metabolic homeostasis in fish kidney [24].

MnSOD is a ubiquitous metalloenzyme that constitutes the front line of antioxidant defense against free radicals [25]. Previous study have demonstrated that MnSOD polypeptide contained 224 residues with a 26 aa long mitochondrial targeting sequence (MTS) and a characteristic motif (DVWEHAYY) in Qihe crucian carp [26]. Current study revealed that the obtained WR-MnSOD encoded 233 amino acid residues, containing a SOD-Fe-N domain, a SOD-Fe-C domain and a conserved characteristic sequence. These results suggested that MnSOD sequences in WR possessed the conserved characteristic sequence with a slight difference in comparison with those of other teleosts. Tissue-specific
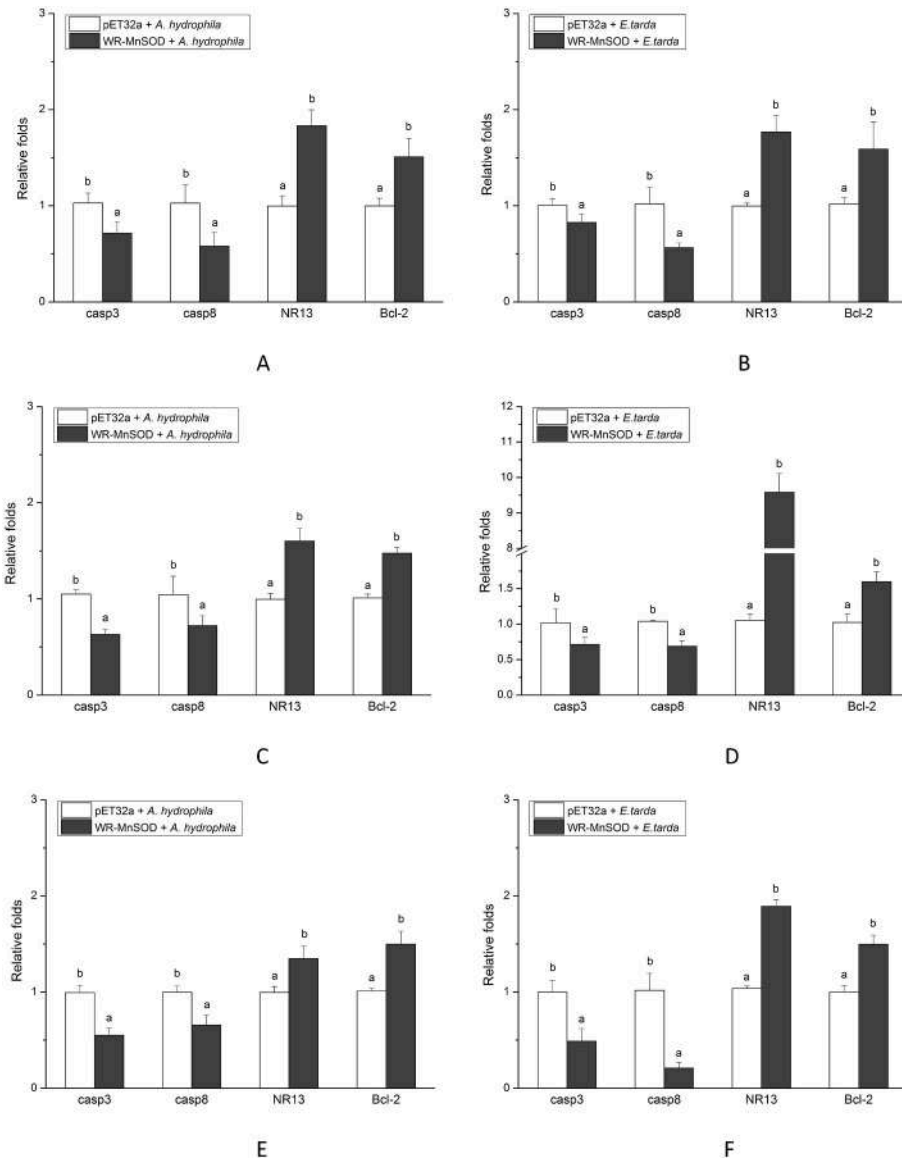
Fig. 8. *In vivo* administration of WR-MnSOD on expressions of apoptotic genes in midgut following *A. hydrophila* and *E. tarda* infection. Expression levels of caspase-3, caspase-8, NR13 and Bcl-2 were determined in midgut (A–B), liver (C–D) and spleen (E–F) of WR. The calculated data (mean ± SD) with different letters were significantly different ($P < 0.05$) among the groups. The experiments were performed in triplicate.

analysis revealed that a high-level mRNA expression of WR-MnSOD was detected in kidney, while the lowest expression was detected in skin, suggesting that the expression of WR-MnSOD mRNA was broadly expressed in various tissues. In general, liver, kidney and spleen play vital roles in fish immunity [27,28]. In this study, elevated expression levels of WR-MnSOD mRNA were detected in liver, kidney and spleen after *A. hydrophila* challenge, indicating that WR-MnSOD may be involved in immune response to *A. hydrophila* infection. However, the study on the gut mucosal barrier function regulated by MnSOD in fish are unclear.

The *in vitro* antioxidant role and expression level of MnSOD were extensively studied in different fish species, including seahorse [12], Qihe crucian carp [26], sterlet [29] and mullet [30], but its regulatory function on gut mucosal immunity remain unclear. In current study, fish receiving *A. hydrophila* infection and *E. tarda* infection were anally intubated with pET32a tag protein and WR-MnSOD protein, respectively. Expression levels of midgut occludin, claudin-7, claudin-8 and claudin-12 increased sharply in WR-MnSOD treatment group, along with elevated levels of goblet cell numbers and length-to-width ratio in midgut villi. In general, tight junction integrity serves as a physiological barrier that can play an important role in the frontline defense against infectious agents [31], while epithelial cells is pivotal sensors of invading microbes in gut tract, which can recruit and chemoattract the adhesion of activated immune cells [32]. Goblet cells distributed in mucus layer coating the gut tract can enable secretion of mucin glycoproteins and other bioactive molecules to participate in the front line of innate immune defense against pathogenic invasion [33]. Additionally, WR-MnSOD treatment could sharply increase expressions of TrxR, OXR1 and TXNL mRNA in midgut subjected to *A. hydrophila* infection and *E. tarda* infection, along with the high-level of CAT, GPx and GR activity. In contrast, a significant decrease of caspase-3 and caspase-8 expression in midgut, liver and spleen in WR-MnSOD + *A. hydrophila* group and WR-MnSOD + *E. tarda* group, while Bcl-2 and NR13 expression increased dramatically. TXNL1 and OXR1 can enable ROS elimination to maintain mitochondrial DNA integrity and affect mitochondrial morphology [34,35], while TrxR inhibition may promote cell death and mitochondrial dysfunction [36]. Indeed, mitochondrial dysfunction is highly linked to up-regulated levels of ROS generation produced by the organelle or endoplasmic reticulum surface [37], which is involved in apoptotic induction [38]. Apoptosis is highly modulated cell death process in the normal development and homeostasis that can enable mounting immunological self-tolerance to confer protection against autoimmunity and aberrant immune response, as well as remodel inflamed sites via phagocytic clearance of dying cells [39,40]. The core effectors of apoptosis encompass caspase family, which can induce apoptotic activation via intrinsic pathway and extrinsic pathway [41], while Bcl-2 and NR13 exert the anti-apoptotic function by blocking caspase activation [42]. Thus, collectively with previous studies, these results firstly suggested that MnSOD could rescue redox balance and counteract oxidative stress in bacteria-infected midgut of hybrid fish, which may maintain gut mucosal barrier function and reduce apoptotic cell death during bacterial infection.

In summary, we characterized the architectures of WR-MnSOD. Then, expression patterns of WR-MnSOD in *A. hydrophila*-infected fish were studied. Gut perfusion with WR-MnSOD fusion protein could confer protein against oxidative stress and maintain high levels of antioxidant status in midgut. In addition, Decreased levels of impaired gut mucosal barrier function and apoptotic gene expressions were observed in midgut following MnSOD treatment. Our results indicated that MnSOD in hybrid fish may play an important role in midgut immune regulation.

Declaration of competing interest

The authors declare that they have no conflict of interest.

References

[1] S.S. Killen, S. Marras, N.B. Metcalfe, D.J. McKenzie, P. Domenici, Environmental stressors alter relationships between physiology and behaviour, Trends Ecol. Evol. 28 (2013) 651–658.

[2] B. Magnadottir, Immunological control of fish diseases, Mar. Biotechnol. 12 (2010) 361–379.

[3] S.A. Kraemer, A. Ramachandran, G.G. Perron, Antibiotic pollution in the environment: from microbial ecology to public policy, Microorganisms 7 (2019) 180.

[4] M. Li, Q-l Wang, Y. Lu, S-l Chen, Q. Li, Z-x Sha, Expression profiles of NODs in channel catfish (Ictalurus punctatus) after infection with Edwardsiella tarda, Aeromonas hydrophila, Streptococcus iniae and channel catfish hemorrhage reovirus, Fish Shellfish Immunol. 33 (2012) 1033–1041.

[5] B. Liu, L. Xu, X. Ge, J. Xie, P. Xu, Q. Zhou, et al., Effects of mannan oligosaccharide on the physiological responses, HSP70 gene expression and disease resistance of Allogynogenetic crucian carp (Carassius auratus gibelio) under Aeromonas hydrophila infection, Fish Shellfish Immunol. 34 (2013) 1395–1403.

[6] M. Yamasaki, K. Araki, K. Maruyoshi, M. Matsumoto, C. Nakayasu, T. Moritomo, et al., Comparative analysis of adaptive immune response after vaccine trials using live attenuated and formalin-killed cells of Edwardsiella tarda in ginbuna crucian carp (Carassius auratus langsdorfii), Fish Shellfish Immunol. 45 (2015) 437–442.

[7] Z. Li, Z.W. Wang, Y. Wang, J.F. Gui, Crucian Carp and Gibel Carp Culture. Aquaculture In China: Success Stories and Modern Trends, 2018, pp. 149–157.

[8] K. Warner, M. Hamza, A. Oliver-Smith, F. Renaud, A. Julca, Climate change, environmental degradation and migration, Nat. Hazards 55 (2010) 689–715.

[9] C. Uribe, H. Folch, R. Enríquez, G. Moran, Innate and adaptive immunity in teleost fish: a review, Vet. Med. 56 (2011) 486.

[10] C. Secombes, T. Wang, S. Hong, S. Peddie, M. Crampe, K. Laing, et al., Cytokines and innate immunity of fish, Dev. Comp. Immunol. 25 (2001) 713–723.

[11] S. Rizwan, P. ReddySekhar, B. MalikAsrar, Reactive oxygen species in inflammation and tissue injury, Antioxidants Redox Signal. (2014).

[12] N. Perera, G. Godahewa, S. Lee, M.-J. Kim, J.Y. Hwang, M.G. Kwon, et al., Manganese-superoxide dismutase (MnSOD), a role player in seahorse (Hippocampus abdominalis) antioxidant defense system and adaptive immune system, Fish Shellfish Immunol. 68 (2017) 435–442.

[13] W.C. Dougall, H.S. Nick, Manganese superoxide dismutase: a hepatic acute phase protein regulated by interleukin-6 and glucocorticoids, Endocrinology 129 (1991) 2376–2384.

[14] H.L. Guo, D. Wolfe, M.W. Epperly, S. Huang, K. Liu, J.C. Glorioso, et al., Gene transfer of human manganese superoxide dismutase protects small intestinal villi from radiation injury, J. Gastrointest. Surg. 7 (2003) 229–236.

[15] Z.-H. Qi, Y.-F. Liu, S.-W. Luo, C.-X. Chen, Y. Liu, W.-N. Wang, Molecular cloning, characterization and expression analysis of tumor suppressor protein p53 from orange-spotted grouper, Epinephelus coioides in response to temperature stress, Fish Shellfish Immunol. 35 (2013) 1466–1476.

[16] G.-H. Cha, S.-W. Luo, Z-h Qi, Y. Liu, W.-N. Wang, Optimal Conditions for Expressing a Complement Component 3b Functional Fragment (α2-Macroglobulin Receptor) Gene from Epinephelus coioides in Pichia pastoris. Protein Expression and Purification, 2015.

[17] C.-H. Cheng, F.-F. Yang, S.-A. Liao, Y.-T. Miao, C.-X. Ye, A.-L. Wang, et al., Identification, characterization and functional analysis of anti-apoptotic protein BCL-2-like gene from pufferfish, Takifugu obscurus, responding to bacterial challenge, Fish Physiol. Biochem. 41 (2015) 1053–1064.

[18] G.P. Morris, P.L. Beck, M.S. Herridge, W.T. Depew, M.R. Szewczuk, J.L. Wallace, Hapten-induced model of chronic inflammation and ulceration in the rat colon, Gastroenterology 96 (1989) 795–803.

[19] F. Wang, Z.L. Qin, W.S. Luo, N.X. Xiong, M.Z. Huang, J. Ou, et al., Alteration of synergistic immune response in gut–liver axis of white crucian carp (Carassius cuvieri) after gut infection with Aeromonas hydrophila, J. Fish. Dis. 00 (2023) 1–11.

[20] C.-H. Cheng, Y.-L. Su, H.-L. Ma, Y.-Q. Deng, J. Feng, X.-L. Chen, et al., Effect of nitrite exposure on oxidative stress, DNA damage and apoptosis in mud crab (Scylla paramamosain), Chemosphere 239 (2020), 124668.

[21] F. Wang, Z.-L. Qin, W.-S. Luo, N.-X. Xiong, S.-W. Luo, Aeromonas hydrophila can modulate synchronization of gut-liver axis of red crucian carp via the breach of gut barrier, Aquacult. Int. (2023) 1–15.

[22] M.K. Jeong, B.-H. Kim, Grading criteria of histopathological evaluation in BCOP assay by various staining methods, Toxicol. Res. 38 (2022) 9–17.

[23] K.J. Davies, Oxidative stress, antioxidant defenses, and damage removal, repair, and replacement systems, IUBMB Life 50 (2000) 279–289.

[24] N.-X. Xiong, Z.-X. Fang, X.-Y. Kuang, J. Ou, S.-W. Luo, S.-J. Liu, Integrated analysis of gene expressions and metabolite features unravel immunometabolic interplay in hybrid fish (Carassius cuvieri♀× Carassius auratus red var♂) infected with Aeromonas hydrophila, Aquaculture 563 (2023), 738981.

[25] M. Berwal, C. Ram, Superoxide dismutase: a stable biochemical marker for abiotic stress tolerance in higher plants, Abiotic biotic stress plants (2018) 1–10.

[26] X. Kong, D. Qiao, X. Zhao, L. Wang, J. Zhang, D. Liu, et al., The molecular characterizations of Cu/ZnSOD and MnSOD and its responses of mRNA expression and enzyme activity to Aeromonas hydrophila or lipopolysaccharide challenge in Qihe crucian carp Carassius auratus, Fish Shellfish Immunol. 67 (2017) 429–440.

[27] C.M. Press, Ø. Evensen, The morphology of the immune system in teleost fishes, Fish Shellfish Immunol. 9 (1999) 309–318.

[28] N.X. Xiong, X.Y. Kuang, Z.X. Fang, J. Ou, S.Y. Li, J.H. Zhao, et al., Transcriptome analysis and co-expression network reveal the mechanism linking mitochondrial function to immune regulation in red crucian carp (Carassius auratus red var) after Aeromonas hydrophila challenge, J. Fish. Dis. 45 (2022) 1491–1509.

[29] A. Sun, H. Zhu, X. Wang, Q. Hu, Z. Tian, H. Hu, Molecular characterization of manganese superoxide dismutase (MnSOD) from sterlet Acipenser ruthenus and its responses to Aeromonas hydrophila challenge and hypoxia stress, Comp. Biochem. Physiol. Mol. Integr. Physiol. 234 (2019) 68–76.

[30] D. Sirisena, N. Perera, G. Godahewa, H. Kwon, H. Yang, B.-H. Nam, et al., A manganese superoxide dismutase (MnSOD) from red lip mullet, Liza haematocheila: evaluation of molecular structure, immune response, and antioxidant function, Fish Shellfish Immunol. 84 (2019) 73–82.

[31] E.E. Schneeberger, R.D. Lynch, The tight junction: a multifunctional complex, Am. J. Physiol. Cell Physiol. 286 (2004) C1213–C1228.

[32] M.F. Kagnoff, L. Eckmann, Epithelial cells as sensors for microbial infection, J. Clin. Investig. 100 (1997) 6–10.

[33] Y.S. Kim, S.B. Ho, Intestinal goblet cells and mucins in health and disease: recent insights and progress, Curr. Gastroenterol. Rep. 12 (2010) 319–330.

[34] M. Yang, L. Luna, J.G. Sørbø, I. Alseth, R.F. Johansen, P.H. Backe, et al., Human OXR1 maintains mitochondrial DNA integrity and counteracts hydrogen peroxide-induced oxidative stress by regulating antioxidant pathways involving p21, Free Radic. Biol. Med. 77 (2014) 41–48.

[35] J.-M. Zhao, T.-G. Qi, The role of TXNL1 in disease: treatment strategies for cancer and diseases with oxidative stress, Mol. Biol. Rep. 48 (2021) 2929–2934.

[36] P. Lopert, B.J. Day, M. Patel, Thioredoxin reductase deficiency potentiates oxidative stress, mitochondrial dysfunction and cell death in dopaminergic cells, PLoS One 7 (2012) e50683.

[37] M.P. Murphy, Mitochondrial dysfunction indirectly elevates ROS production by the endoplasmic reticulum, Cell Metabol. 18 (2013) 145–146.

[38] J.D. Ly, D. Grubb, A. Lawen, The mitochondrial membrane potential (Δψm) in apoptosis; an update, Apoptosis 8 (2003) 115–128.

[39] M. Chen, Y.-H. Wang, Y. Wang, L. Huang, H. Sandoval, Y.-J. Liu, et al., Dendritic cell apoptosis in the maintenance of immune tolerance, Science 311 (2006) 1160–1164.

[40] J. Savill, Apoptosis in resolution of inflammation, J. Leukoc. Biol. 61 (1997) 375–380.

[41] K.M. Boatright, G.S. Salvesen, Mechanisms of caspase activation, Curr. Opin. Cell Biol. 15 (2003) 725–731.

[42] E. Kratz, P. Eimon, K. Mukhyala, H. Stern, J. Zha, A. Strasser, et al., Functional characterization of the Bcl-2 gene family in the zebrafish, Cell Death Differ. 13 (2006) 1631–1640.